CELL BIOLOGY

# VRK-1 extends life span by activation of AMPK via phosphorylation

**Sangsoon Park[1]*, Murat Artan[1]*†, Seung Hyun Han[2]*, Hae-Eun H. Park[3], Yoonji Jung[3], Ara B. Hwang[1]‡, Won Sik Shin[2], Kyong-Tai Kim[1,2]§, Seung-Jae V. Lee[3]§**



**Vaccinia virus–related kinase (VRK) is an evolutionarily conserved nuclear protein kinase. VRK-1, the single *Caenorhabditis elegans* VRK ortholog, functions in cell division and germline proliferation. However, the role of VRK-1 in postmitotic cells and adult life span remains unknown. Here, we show that VRK-1 increases organismal longevity by activating the cellular energy sensor, AMP-activated protein kinase (AMPK), via direct phosphorylation. We found that overexpression of *vrk-1* in the soma of adult *C. elegans* increased life span and, conversely, inhibition of *vrk-1* decreased life span. In addition, *vrk-1* was required for longevity conferred by mutations that inhibit *C. elegans* mitochondrial respiration, which requires AMPK. VRK-1 directly phosphorylated and up-regulated AMPK in both *C. elegans* and cultured human cells. Thus, our data show that the somatic nuclear kinase, VRK-1, promotes longevity through AMPK activation, and this function appears to be conserved between *C. elegans* and humans.**

## INTRODUCTION

Mitochondria are essential subcellular organelles for cellular energy production [reviewed in (*1*)]. Mitochondria also play important functions in a wide array of other cellular processes, ranging from cellular signaling to apoptosis. In addition, mitochondria play crucial roles in organismal aging, and functional declines in mitochondria are associated with age-related diseases [reviewed in (*2*)]. However, mild inhibition of mitochondrial respiration has been shown to promote longevity in multiple species [reviewed in (*3*)]. In *Caenorhabditis elegans*, the genetic inhibition of mitochondrial respiration genes, including *isp-1* (Rieske iron-sulfur protein in complex III) and *clk-1* (coenzyme Q biosynthesis enzyme crucial for electron transport), prolongs life span. Inhibition of mitochondrial respiration also increases life span in *Drosophila* and mammals. Therefore, life-span extension by reduced mitochondrial respiration is conserved, and the elucidation of the molecular mechanism in *C. elegans* may enhance our understanding of human aging and longevity.

Adenosine 5′-monophosphate (AMP)–activated protein kinase (AMPK), a critical cellular energy sensor that increases life span in multiple species [reviewed in (*4*)], is one of the factors required for the enhanced longevity caused by inhibition of mitochondrial respiration in *C. elegans* (*5*–*7*). AMPK is activated by an elevated AMP/adenosine 5′-diphosphate (ADP)–to–adenosine 5′-triphosphate (ATP) ratio that results from reduced cellular energy, leading to increases in catabolic processes and inhibition of anabolic processes [reviewed in (*8*)]. Activation of AMPK results from phosphorylation at residue $Thr^{172}$ in its catalytic α subunit by upstream kinases. Liver kinase B1 (LKB1) and $Ca^{2+}$/calmodulin-dependent protein kinase kinase β (CaMKKβ) are two kinases that function to activate AMPK in mammals [reviewed in (*9*)]. Transforming growth factor–β–activated kinase 1 (TAK1) has also been shown to phosphorylate AMPK in vitro [reviewed in (*9*)]. However, the upstream regulators of AMPK that facilitate its life span–extending effects remain incompletely understood.

The vaccinia virus–related kinase (VRK) family consists of three serine-threonine protein kinases (VRK1 to VRK3) in mammals, which are related to casein kinases (*10*–*12*). Among these three, the best characterized is VRK1, a cell cycle regulator that is abundant in proliferative tissues (*13*). Unlike mammals, *C. elegans* has a single VRK ortholog, VRK-1, whose function in cell proliferation is relatively well established (*14*–*16*). Strong loss-of-function mutations of the *C. elegans vrk-1* gene results in sterility, and reduced *vrk-1* function leads to mislocalization of barrier-to-autointegration factor 1 (BAF-1), a phosphorylation target of VRK-1, resulting in severe mitotic defects (*15*, *17*, *18*). *vrk-1* is also required for germ cell proliferation, likely through its ability to regulate the p53-like protein, *C. elegans* p53-like-1 (CEP-1) (*16*), and plays important roles in the development of vulva and uterus (*17*, *18*). However, it remains unknown whether VRK-1 acts in postmitotic cells or has a role in adult life span.

In this study, we sought to elucidate the role of VRK-1 in regulation of adult life span in *C. elegans*. We found that overexpression of VRK-1::GFP (green fluorescent protein), which was detected in the nuclei of cells in multiple somatic tissues, including the intestine, increased life span. Conversely, genetic inhibition of *vrk-1* decreased life span. We further showed that *vrk-1* was essential for the increased life span of mitochondrial respiratory mutants. We demonstrated that VRK-1 was responsible for increasing the level of active and phosphorylated form of AMPK (p-AMPK). In addition, we found that mammalian VRK1 directly phosphorylated AMPK at $Thr^{172}$, resulting in its increased activity. Together, these data indicate that the nuclear protein kinase, VRK-1, which acts in somatic cells, promotes longevity by increasing the activity of AMPK through phosphorylation.

## RESULTS

### Nuclear expression of VRK-1 in somatic tissues extends *C. elegans* life span

To determine the role of *vrk-1* in regulating adult life span, we generated transgenic *C. elegans* overexpressing *vrk-1* fused with the *GFP* gene

[1]Department of Life Sciences, Pohang University of Science and Technology, Pohang, Gyeongbuk 37673, South Korea. [2]Division of Integrative Biosciences and Biotechnology, Pohang University of Science and Technology, Pohang, Gyeongbuk 37673, South Korea. [3]Department of Biological Sciences, Korea Advanced Institute of Science and Technology, Daejeon 34141, South Korea.
*These authors contributed equally to this work.
†Present address: Institute of Science and Technology (IST) Austria, Am Campus 1, Klosterneuburg 3400, Austria.
‡Present address: Memphis Meats Inc., P.O. Box 3468, Berkeley, CA 94703, USA.
§Corresponding author. Email: seungjaevlee@kaist.ac.kr (S.-J.V.L.); ktk@postech.ac.kr (K.-T.K.)

(*vrk-1::GFP*). The VRK-1::GFP was predominantly localized to the nuclei of many cells, including neural, intestinal, and hypodermal cells (Fig. 1A and fig. S1, A and B) (*16*–*18*). In addition, we found that VRK-1::GFP was highly expressed throughout the *C. elegans* life cycle, in the soma of larvae (Fig. 1A and fig. S1, A and B) and fully grown adult worms (Fig. 1B and fig. S1C), comprising postmitotic cells after the cells stopped dividing. Notably, extrachromosomal transgenes that overexpress *vrk-1::GFP*, which is limited to somatic cells because of transgene silencing in germ cells (*19*), substantially increased adult life span (Fig. 1, C and D, and fig. S2A). We then confirmed the longevity conferred by overexpression of *vrk-1::GFP* using an integrated transgenic line (Fig. 1, E and F, and fig. S2B). These data suggest that *vrk-1* overexpression specifically in somatic cells promotes the longevity of *C. elegans*.

We next investigated the effect of *vrk-1* inhibition on the life span of *C. elegans*. *vrk-1* RNA interference (RNAi) and strong loss-of-function mutation *vrk-1(ok1181)* (fig. S2G) (*15*–*17*) shortened *C. elegans* life span (Fig. 1, G and H, and fig. S2, E and F). These results indicate that *vrk-1* is required for the maintenance of normal life span. Together, these data indicate that VRK-1 is necessary and sufficient for longevity.

## VRK-1 contributes to the longevity of mitochondrial respiration mutants

We then asked whether VRK-1 played a role in the increased life span conferred by various mutations in *C. elegans*. RNAi knockdown of *vrk-1* largely suppressed the longevity conferred by mutations in

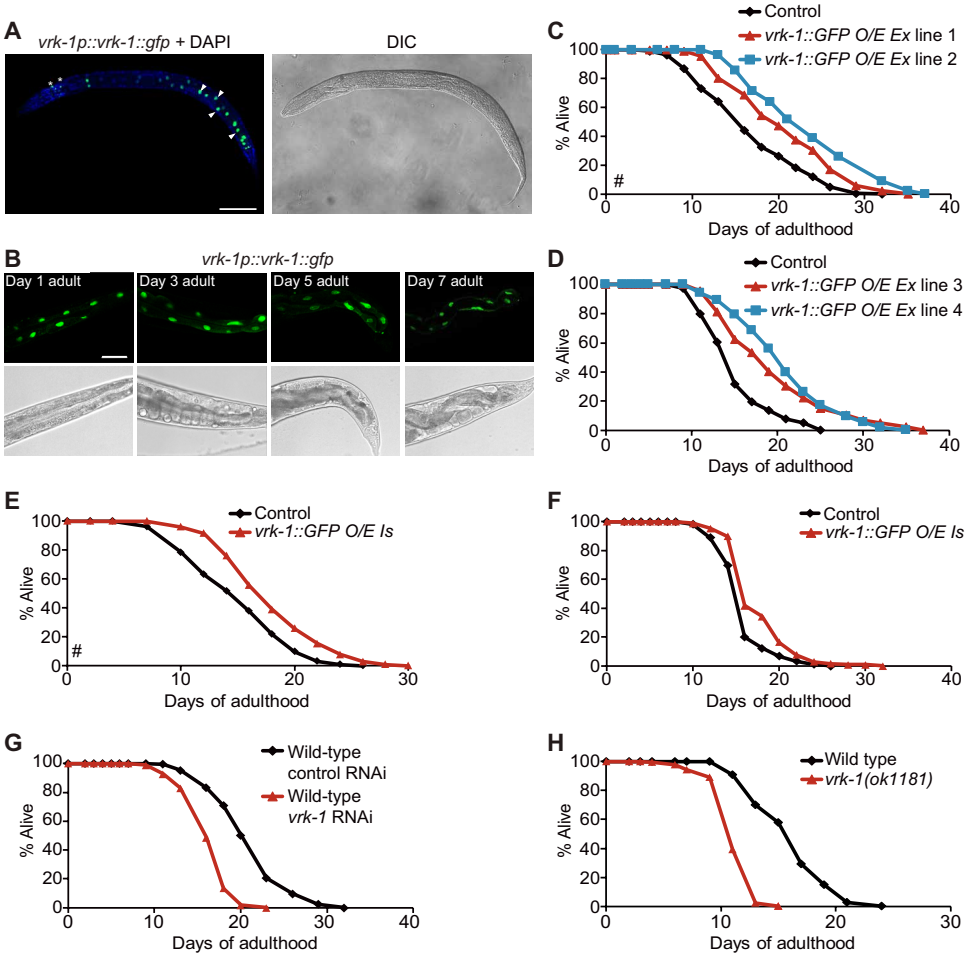


**Fig. 1. VRK-1 is a nuclear protein that increases worm life span.** (**A**) VRK-1::GFP was localized in the cellular nuclei of multiple tissues including neurons (asterisks), intestine (arrowheads), and hypodermis (fig. S1B, arrows) at L2 larval stage. Nuclear DNA was stained with 4′,6-diamidino-2-phenylindole (DAPI; blue). See also fig. S1 (A and B) for magnified images of VRK-1::GFP and cellular nuclei for specific tissues. DIC, differential interference contrast. Photo credit: Sangsoon Park, Pohang University of Science and Technology, South Korea. (**B**) VRK-1::GFP was expressed in somatic tissues of days 1, 3, 5, and 7 adult worms. Scale bars, 50 μm. Photo credit: Murat Artan, MRC Laboratory of Molecular Biology, UK. (**C** and **D**) Four independent lines of extrachromosomal *vrk-1::GFP*-transgenic worms (*vrk-1::GFP O/E Ex*) displayed increased life span with [(C), fig. S2A, transgenic lines 1 to 4] or without (D, transgenic lines 3 and 4) 5-fluoro-2′-deoxyuridine (FUDR) treatment. *odr-1p::RFP* (C) and *rol-6D* (D) were used as coinjection markers, and *odr-1p::RFP* (C) and *rol-6D* (D) transgenic worms were used as controls, respectively. We found that germline-specific transgenic expression of *pie-1p::GFP::vrk-1* (*16*) had no effect on life span (fig. S2, C and D). VRK-1 tagged with GFP appears to be functional because previous reports have shown that GFP::VRK-1 transgenes rescued the sterility, uterine and uterine seam cell developmental defects, and protruding vulva phenotypes of *vrk-1* mutants (*16*–*18*). (**E** and **F**) An integrated *vrk-1::GFP* transgenic line (*vrk-1::GFP Is*) extended life span with [(E), four of five trials] or without [(F), three of three trials] FUDR treatment. Control indicates wild-type N2. (**G**) *vrk-1* RNAi significantly shortened life span. See also fig. S2E for life-span results of *vrk-1(RNAi)* animals treated with FUDR. (**H**) *vrk-1(ok1181)* mutation substantially shortened life span without FUDR treatment. In contrast, hypomorphic *vrk-1(x1)* mutants had a life span similar to that of wild-type worms (fig. S2, H and I). # indicates life-span results that were obtained with FUDR treatment to prevent progeny from hatching. See also table S1 for values and statistical analysis for the life-span data.

mitochondrial respiration genes, *isp-1* (Fig. 2A and fig. S3, A to C) and *clk-1* (Fig. 2B). Similarly, the *vrk-1(ok1181)* mutation suppressed the long life span of *isp-1* mutants (Fig. 2C). We then found that genetic inhibition of *vrk-1* by RNAi or by the deletion mutation, *vrk-1(ok1181)*, decreased the longevity of insulin/insulin-like growth factor 1 receptor *daf-2(−)* mutants (Fig. 2, D and E). In addition, *vrk-1* RNAi shortened the life span of dietary restriction mimetic *eat-2(−)* (Fig. 2F) and hypoxia-inducible factor 1 (HIF-1)–hyperactive *vhl-1(−)* (Fig. 2G) mutants as well as RNAi-mediated electron transport chain–inhibited *cco-1(RNAi)* animals (fig. S3, F to H; see Fig. 2 legends for discussion). Together, these data suggest that *vrk-1* contributes to longevity conferred by various longevity interventions and, in particular, is essential for that caused by the inhibition of mitochondrial respiration.

## VRK-1 regulates expression of AMPK target genes

We next investigated the mechanism by which VRK-1 contributed to the longevity of mitochondrial respiration mutants. To this end, we first determined whether inhibition of nuclear protein VRK-1 affected gene expression in *isp-1(−)* mutants by performing mRNA sequencing (mRNA-seq) analysis. We identified 1589 up-regulated and 199 down-regulated genes in *isp-1(−)* mutants versus wild-type worms (fold change > 2 and < 0.5, $P < 0.001$; Fig. 3A and data file S1). Among these differentially expressed genes (DEGs), the expression of 328 up-regulated genes and 22 down-regulated genes was dependent on *vrk-1* (Fig. 3A and data file S1). Gene Ontology (GO) analysis indicated that genes involved in diverse biological processes were enriched among *vrk-1*–dependent up-regulated genes

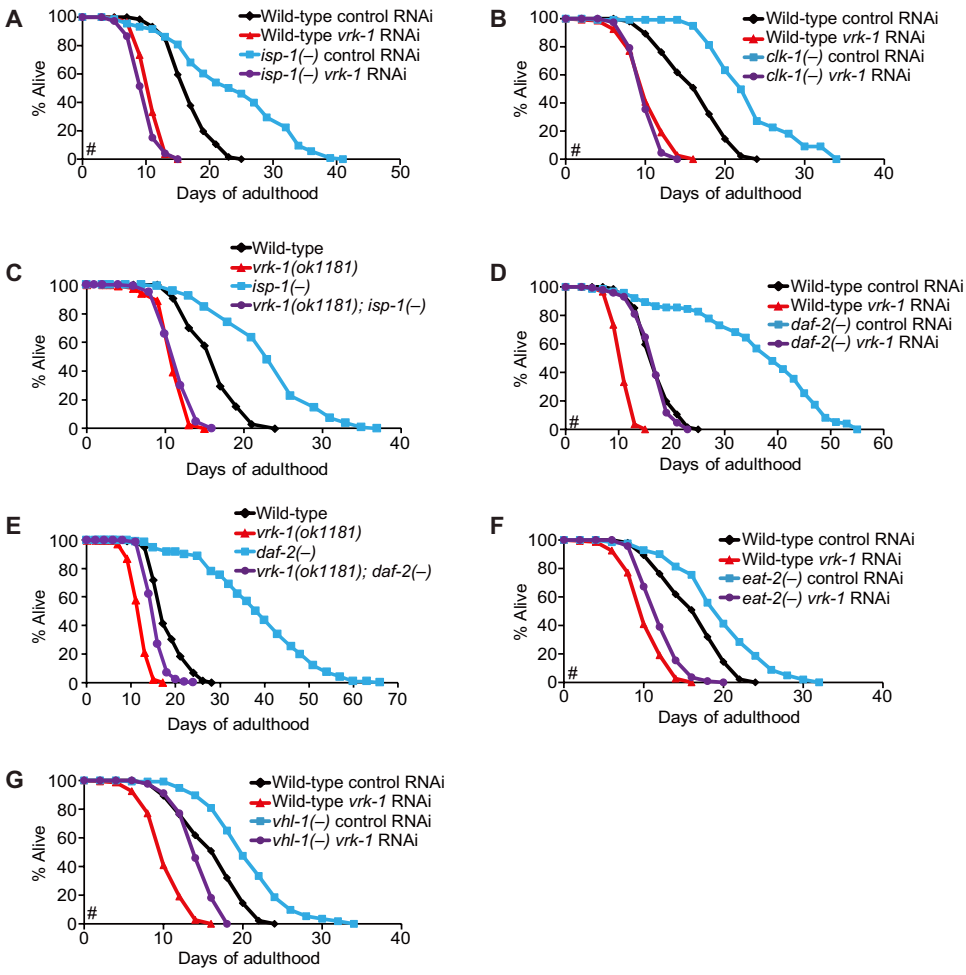


**Fig. 2. Inhibition of VRK-1 suppresses the longevity of mitochondrial respiration mutants.** (**A** and **B**) *vrk-1* RNAi suppressed the long life span of *isp-1(qm150)* [*isp-1(−)*] (A) and *clk-1(qm30)* [*clk-1(−)*] (B) mutants. *vrk-1* RNAi partially but substantially suppressed the longevity of *isp-1(−)* mutants without FUDR treatment (fig. S3A). Quantitative reverse transcription polymerase chain reaction (qRT-PCR) analysis confirmed that *vrk-1* RNAi decreased *vrk-1* mRNA level for the life-span assays (fig. S3, B and C). Different from mitochondrial respiration mutants, longevity caused by inhibition of mitochondrial respiration using *cco-1* RNAi knockdown (*39*, *40*) was indiscriminately decreased by *vrk-1* RNAi (fig. S3F). Our data are consistent with previous reports showing that mutation and RNAi of mitochondrial electron transport chain components distinctly promote longevity by acting with different factors [reviewed in (*3*)]. (**C**) A strong loss-of-function *vrk-1(ok1181)* mutation suppressed the long life span of *isp-1(−)* mutants without FUDR treatment. In addition, *vrk-1(x1)* mutation substantially reduced the long life span of *isp-1(−)* mutants (fig. S3D). (**D** and **E**) *vrk-1* RNAi (D) or *vrk-1(ok1181)* mutation (E) substantially reduced the life span of *daf-2(e1370)* [*daf-2(−)*] mutants. (**F** and **G**) Knockdown of *vrk-1* shortened the life span of *eat-2(ad1116)* [*eat-2(−)*] (F) and *vhl-1(ok161)* [*vhl-1(−)*] (G) mutants, similarly to that of wild type. Hypomorphic *vrk-1(x1)* mutation did not reduce the long life span of *daf-2(−)* (fig. S3E), *eat-2(−)* (fig. S3I), or *osm-5(−)* (fig. S3J) animals. # indicates life-span results obtained with FUDR treatment to prevent progeny from hatching. See also table S1 for values and statistical analysis for life-span data.

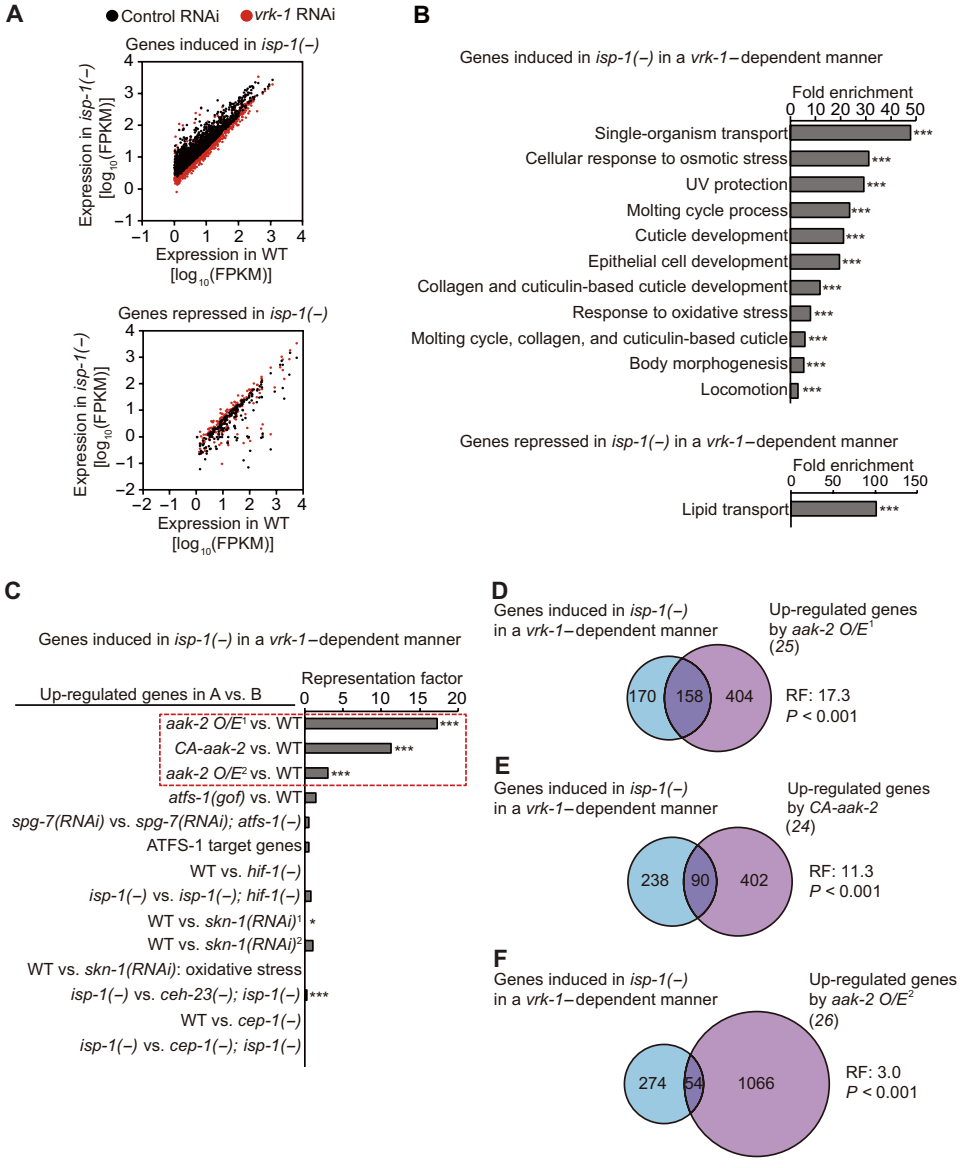


**Fig. 3. Genes up-regulated by *isp-1(–)* in a *vrk-1*–dependent manner overlap with AMPK–up-regulated genes.** (**A**) *vrk-1* RNAi suppressed the *isp-1(–)*–mediated induction and repression of a subset of genes. Black dots indicate mean FPKM (fragments per kilobase of transcript per million mapped reads) of genes that were up- or down-regulated by *isp-1(–)* under a control RNAi condition [fold change, >2 (top) or <0.5 (bottom); $P < 0.001$]. Red dots indicate mean FPKM of the genes in *isp-1(–)* treated with *vrk-1* RNAi compared to wild type (WT) treated with control RNAi. See also data file S1. (**B**) Biological process GO terms that were enriched among genes up- or down-regulated by *isp-1(–)* in a *vrk-1*–dependent manner (***$P < 0.001$). UV, ultraviolet. (**C** to **F**) Genes up-regulated by *isp-1(–)* in a *vrk-1*–dependent manner were enriched for genes up-regulated by AMPK. Genes that were induced in *isp-1(–)* animals in a *vrk-1*–dependent fashion were analyzed to calculate overlaps and representation factor (RF) with published transcriptome data by using WormExp (*$P < 0.05$ and ***$P < 0.001$) (see Materials and Methods). *aak-2 O/E*[1] and *aak-2 O/E*[2]: genes up-regulated by *aak-2* overexpression from two different transcriptome data (C, D, and F). *CA-aak-2:* genes up-regulated by constitutively active (*CA*) *aak-2* (C and E). *atfs-1(gof):* an *atfs-1(et18)* gain-of-function mutant (C). *spg-7(RNAi)*: a condition that induces mitochondrial stress and activates ATFS-1. ATFS-1 target genes: genes whose promoter regions bind ATFS-1 in *spg-7(RNAi)* animals (C). *skn-1(RNAi)*[1] and *skn-1(RNAi)*[2]: genes down-regulated by *skn-1(RNAi)* from two different transcriptome data (C). "WT vs. *skn-1(RNAi)*: oxidative stress" indicates genes down-regulated by *skn-1(RNAi)* under oxidative stress conditions. See also fig. S4 for details.

in *isp-1(–)* mutants, whereas those involved in lipid transport were enriched among the down-regulated genes (Fig. 3B).

We then asked which factors functioned in conjunction with VRK-1 to affect gene expression changes in mitochondrial respiration-defective mutants. We compared the *vrk-1*–dependent DEGs in *isp-1(–)* mutants with those regulated by respiration mutation-mediated longevity factors, including AMP-activated kinase 2 (AAK-2)/AMPK, activating transcription factor associated with stress–1 (ATFS-1)/basic leucine zipper transcription factor required for mitochondrial unfolded protein response, HIF-1, SKN-1, *C. elegans* homeobox 23 (CEH-23), and CEP-1 [WormExp (*20*)]. Genes whose induction was dependent on *vrk-1* in *isp-1(–)* mutants displayed the most significant overlap with those up-regulated by AMPK (Fig. 3, C to F). In contrast, transcriptomic comparison with ATFS-1,

HIF-1, SKN-1, CEH-23, or CEP-1 did not yield a substantial overlap (Fig. 3C and fig. S4).

We then performed quantitative reverse transcription polymerase chain reaction (qRT-PCR) analysis to measure the expression levels of *vrk-1*–dependent genes induced in *isp-1(−)* mutants (*21*–*23*) and positively regulated by AMPK (*24*–*26*) (Fig. 4, A and B). Of the 14 genes that we analyzed, most were up-regulated by the *isp-1* mutation in an AMPK-dependent manner (Fig. 4A). Consistent with our RNA sequencing (RNA-seq) results (fig. S5A), we also found that expression of these putative AMPK target genes was decreased by *vrk-1* RNAi in *isp-1* mutants (Fig. 4B). Moreover, down-regulation of the tested *isp-1(−)*–dependent AMPK target genes by *aak-2(−)* mutation was not additive to that by *vrk-1* RNAi (fig. S5B). These results support the hypothesis that *vrk-1* mediates the up-regulation of AMPK-dependent genes. In contrast, RNAi knockdown of *vrk-1* did not suppress the induction of *hsp-6p::GFP* (ATFS-1 reporter), *nhr-57p::GFP* (HIF-1 reporter), *gst-4p::GFP* (SKN-1 reporter), or *ceh-23* in *isp-1(−)* mutants (Fig. 4, C to F, and fig. S5, C to E). Together, these data suggest that VRK-1 induces a large subset of genes that are regulated by AMPK in long-lived mitochondrial respiration mutants.

## VRK-1 promotes life extension by up-regulating AMPK, thereby down-regulating CRTC-1

We further determined the relationship between VRK-1 and AMPK in the regulation of *C. elegans* longevity. We first confirmed that genetic inhibition of *aak-2/AMPK* partially suppressed the long life span of *isp-1* mutants (Fig. 5A and fig. S6A), consistent with previous reports (*5*, *6*). We found that *vrk-1* RNAi slightly decreased the life span of *isp-1(−); aak-2(−)* mutants (Fig. 5B and fig. S6, B and C). These data raise the possibility that *vrk-1* has an additional life

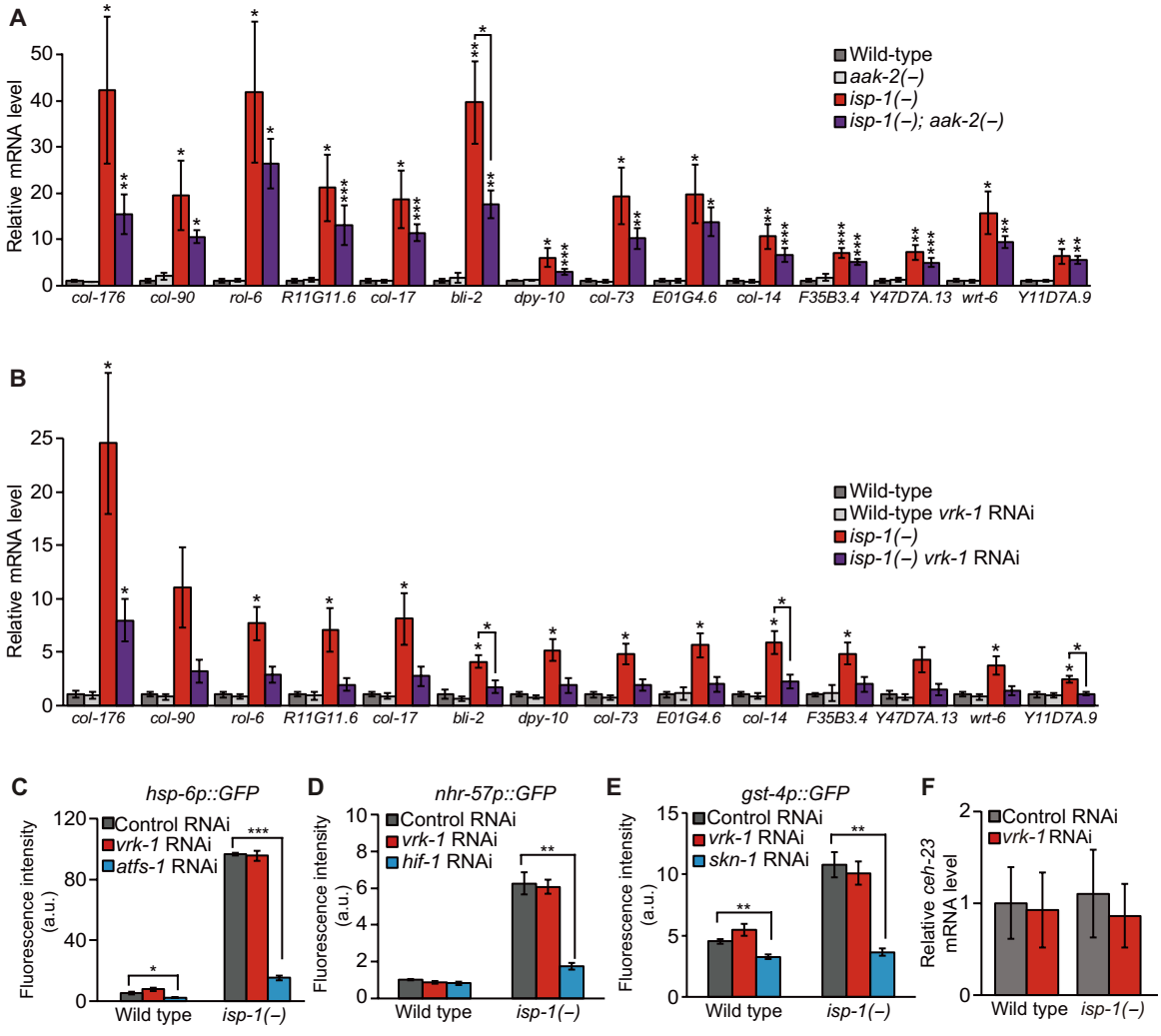


**Fig. 4. Knockdown of *vrk-1* decreases AMPK target gene expression in *isp-1* mutants.** (**A** and **B**) qRT-PCR analysis. The expression of many selected genes that were up-regulated by *isp-1(−)* mutation was reduced by *aak-2(−)* mutation [(A), $n = 5$]. The majority of genes up-regulated by *isp-1(−)* in (A) were also suppressed by *vrk-1* RNAi [(B), $n = 3$]. See fig. S7A for AMPK target gene expression changes caused by food deprivation (FD) and *vrk-1* RNAi. Error bars represent SEMs (*$P < 0.05$, **$P < 0.01$, and ***$P < 0.001$, two-tailed Student's *t* test). See also fig. S5A for the expression changes of genes shown in (A) and (B) by *isp-1(−)* and *vrk-1* RNAi from our RNA-seq data. (**C** to **E**) *vrk-1* RNAi did not alter the expression of *hsp-6p::GFP* (C), *nhr-57p::GFP* (D), or *gst-4p::GFP* (E) in wild-type or *isp-1(−)* animals ($n = 3$, >60 animals). Fluorescence intensities indicate average pixel intensities of fluorescence shown as arbitrary units (a.u.). Error bars represent SEMs (*$P < 0.05$, **$P < 0.01$, and ***$P < 0.001$, two-tailed Student's *t* test). *atfs-1* RNAi (C), *hif-1* RNAi (D), and *skn-1* RNAi (E) were used as positive controls. See also fig. S5 (C to E) for representative images. (**F**) *vrk-1* RNAi did not influence the expression of *ceh-23* mRNA in wild-type or *isp-1(−)* animals measured by using qRT-PCR ($n = 3$). Error bars represent SEMs.

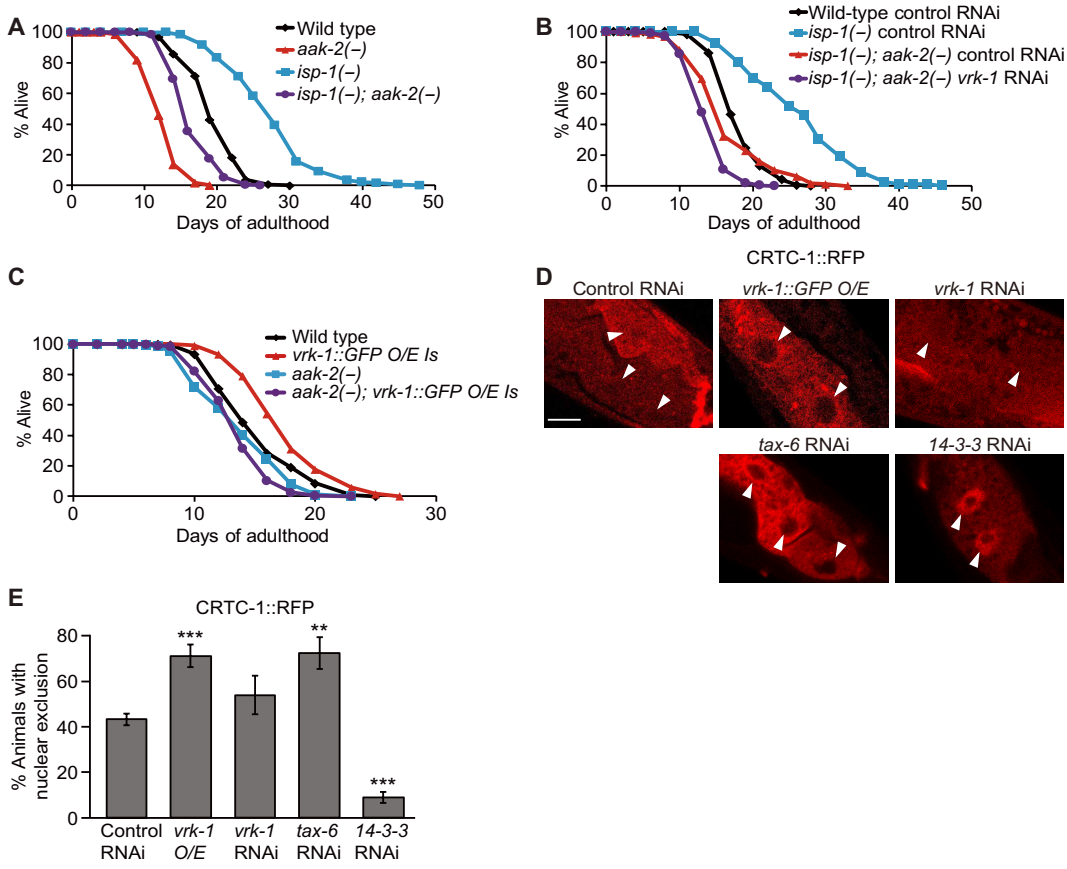


**Fig. 5. VRK-1 mediates longevity in mitochondrial mutants by acting together with AMPK and CRTC-1.** (**A**) *aak-2(ok524)* [*aak-2(–)*] mutation partially suppressed the long life span of *isp-1(–)* mutants without FUDR. (**B**) *vrk-1* RNAi slightly but significantly decreased the life span of *isp-1(–); aak-2(–)* double mutants without FUDR. qRT-PCR analysis confirmed that *vrk-1* RNAi decreased *vrk-1* mRNA level for the life-span assays (fig. S6C). (**C**) *aak-2(–)* mutation suppressed long life span conferred by an integrated transgene of *vrk-1::GFP* [*vrk-1::GFP O/E Is*] (two of three trials) without FUDR. See also fig. S6 (A, B, and D) for life-span assays with FUDR treatment. See also table S1 for values and statistical analysis for life-span data. (D and E) Nuclear exclusion of CRTC-1::RFP was increased by *vrk-1::GFP O/E* but was not affected by *vrk-1* RNAi. (**D**) Representative images of CRTC-1::RFP. *tax-6* RNAi and *14-3-3* RNAi (*par-5* and *ftt-2* double RNAi) that increased and decreased the nuclear exclusion of CRTC-1::RFP, respectively (*26*), were used as positive controls. Arrowheads indicate the nuclei of intestinal cells. Scale bar, 10 μm. See also fig. S6J for representative images of CRTC-1::RFP with nuclear DNA stained with DAPI (blue). Photo credit: Sangsoon Park, Pohang University of Science and Technology, South Korea. (**E**) Percent animals with CRTC-1::RFP nuclear exclusion ($n = 6$, >87 animals). Error bars represent SEMs (*$P < 0.05$ and **$P < 0.01$, two-tailed Student's $t$ test). See fig. S6 (E to I) for qRT-PCR analysis results showing RNAi knockdown efficiency. See also fig. S7 (B and C) for CRTC-1::RFP localization change by food deprivation and *vrk-1::GFP O/E*.

span–regulatory function that is independent of AMPK. We then performed the converse experiment using *vrk-1::GFP*-overexpressing animals and showed that *aak-2/AMPK* was required for the long life span of *vrk-1::GFP*-overexpressing animals (Fig. 5C and fig. S6D). Thus, VRK-1 appears to promote longevity in mitochondrial respiration mutants by acting at least partially through AMPK.

Previous reports have shown that AMPK promotes longevity by phosphorylating CRTC-1 (cyclic AMP response element–binding protein–regulated transcriptional coactivator 1) and subsequently promoting its nuclear exclusion (*24*, *26*). We found that *vrk-1::GFP O/E* increased the nuclear exclusion of CRTC-1::RFP (Fig. 5, D and E, and fig. S6J), raising the possibility that VRK-1 overexpression promotes longevity through regulating CRTC-1 via AMPK activation. However, converse experiments using *vrk-1* RNAi were negative (Fig. 5, D and E, and fig. S6J), and therefore, inhibition of *vrk-1* does not seem to be sufficient to affect the CRTC-1 activity. Overall, up-regulation of VRK-1 may promote longevity, at least in part, acting via the AMPK–CRTC-1 signaling axis.

## VRK1 increases the activity of AMPK via phosphorylation

We next asked how VRK-1 up-regulated AMPK target gene expression to promote longevity. Because both VRK-1 and AMPK are protein kinases, we tested whether VRK-1 regulated AMPK activity through phosphorylation. Using cultured human cells, we found that the levels of human phospho-AMPK (p-AMPKα) were increased by overexpression of human *VRK1* (Fig. 6A) and reduced by small interfering RNA (siRNA)–mediated *VRK1* knockdown (Fig. 6B). By using coimmunoprecipitation assays, we showed the physical interaction between endogenous VRK1 and AMPKα2 (Fig. 6C) as well as Flag-AMPK and VRK1 (Fig. 6D and fig. S8D). Overexpression of VRK1 also increased the level of phosphorylated AMPKα (p-AMPKα) in the immunoprecipitated fraction (Fig. 6D). These data suggest a weak and transient interaction between the kinase (VRK1) and its substrate (AMPK).

We then performed in vitro kinase assays with recombinant AMPKα2 and VRK1 to determine whether VRK1 can directly phosphorylate AMPK (Fig. 6, E and F). We found that VRK1 increased

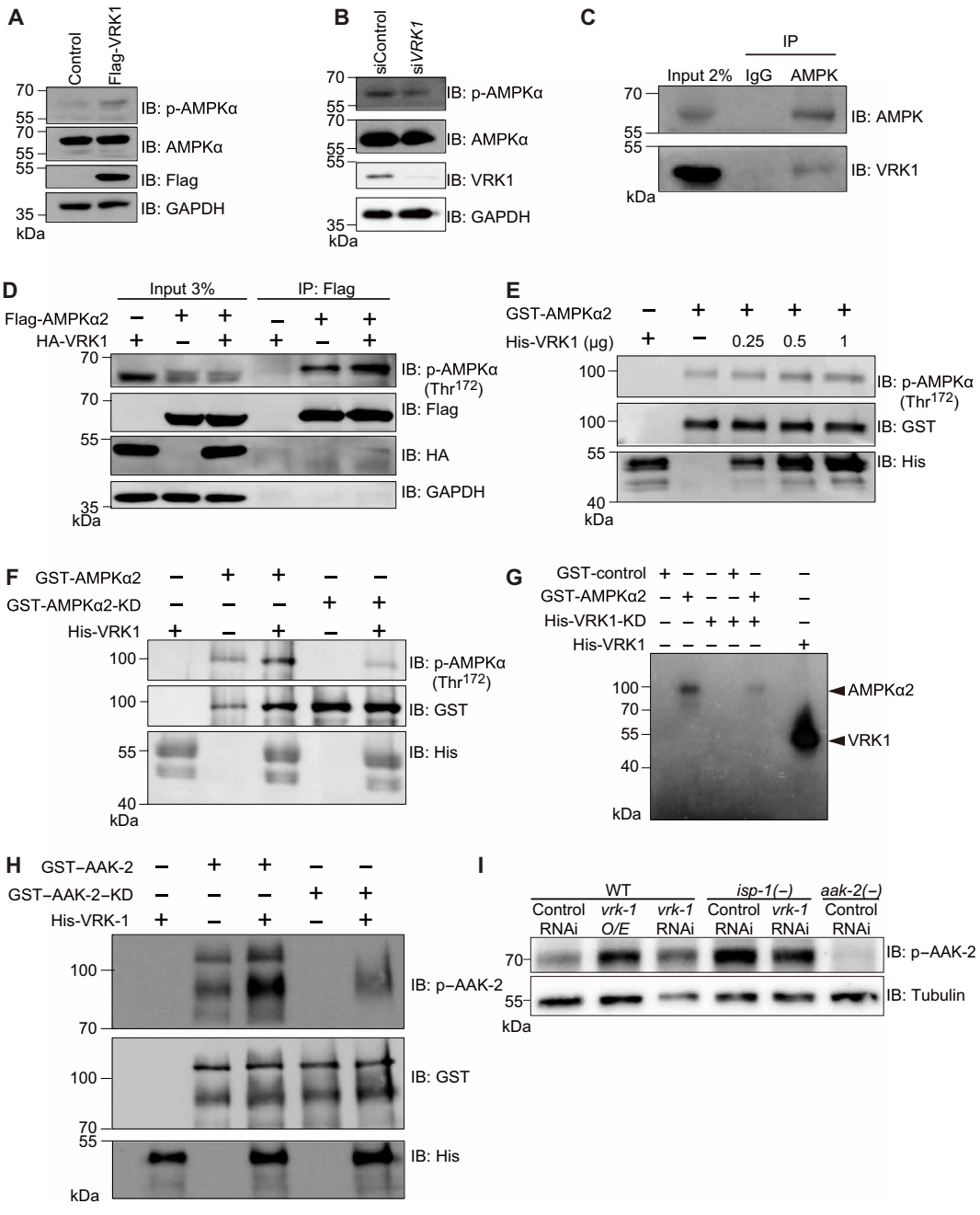


**Fig. 6. VRK-1 increases the activity of AMPK through direct phosphorylation.** (**A** and **B**) Western blot analysis of the p-AMPKα (Thr$^{172}$) in cultured human cells showed that overexpression of human *VRK1* increased p-AMPKα levels in U2OS human osteosarcoma cells ($n = 3$) (A). Control indicates the expression of a Flag-containing vector. Conversely, knockdown of *VRK1* by using siRNA decreased the p-AMPKα levels in SK-HEP-1 human liver endothelial cells ($n = 3$) (B). p-AMPKα/AMPKα ratio indicates the relative intensity of endogenous p-AMPKα (Thr$^{172}$) signal with respect to that of AMPKα. (**C**) Endogenous VRK1 was coimmunoprecipitated with endogenous AMPK ($n = 3$). Antibody against immunoglobulin G (IgG) was used as a negative control for immunoprecipitation. (**D**) VRK1 weakly bound AMPK and up-regulated AMPK. VRK1 increased the level of p-AMPKα2 and was coimmunoprecipitated with AMPKα2 ($n = 3$). Flag- or HA-containing empty vectors were used as negative controls for immunoprecipitation. Glyceraldehyde-3-phosphate dehydrogenase (GAPDH) was used as a loading control. IP, immunoprecipitation; IB, immunoblot. (**E** and **F**) In vitro kinase assay showed that p-AMPKα (Thr$^{172}$) level was increased with the addition of VRK1 in a dose-dependent manner ($n = 3$) (E), and the increase in p-AMPKα level by VRK1 was independent of the autophosphorylation activity of AMPKα2 ($n = 6$) (F). We did not observe a substantial change in p-AMPKα levels in wild-type AMPK by VRK1 (0.5 μg), possibly because of strong autophosphorylation activity of AMPK, which may interfere with phosphorylation by VRK1. (**G**) Radioactive in vitro kinase assay of AMPK and VRK1-KD showed that AMPK did not phosphorylate VRK1 ($n = 4$). No radioactive signal from VRK1 was detected when AMPKα2 was coincubated with VRK-1–KD (lane 5), compared to a robust autophosphorylation signal by wild-type VRK1 (lane 7). Lane 6, protein size marker. (**H**) In vitro kinase assay using recombinant *C. elegans* VRK-1 and AAK-2 isoform b showed that VRK-1 phosphorylated AAK-2–KD ($n = 3$). p–AAK-2 was detected by using mammalian p-AMPKα (Thr$^{172}$) antibody (see Materials and Methods). (**I**) *vrk-1::GFP O/E* increased the p–AAK-2 levels, and *vrk-1* RNAi decreased p–AAK-2 levels in *isp-1(–)* animals, which displayed elevated p–AAK-2 levels ($n = 4$). See also fig. S8 for uncropped Western blot images and fig. S9 for the quantification of independent experiments.

the level of AMPKα phosphorylation at Thr$^{172}$, a known phosphorylation site for activation, in a dose-dependent manner (Fig. 6E). Because we detected substantial autophosphorylation of AMPKα2 (Fig. 6E, lane 2, and Fig. 6F, lane 2), we used a kinase-dead (KD) form of AMPKα2 (AMPKα2-KD) and found that VRK1 phosphorylated AMPKα2–KD (Fig. 6F, lane 5). In contrast, AMPKα2 did not phosphorylate a KD form of VRK1 (VRK1-KD) in vitro (Fig. 6G). These data indicate that VRK1 can directly phosphorylate AMPK but reverse does not occur. By using in vitro kinase assay, we showed that *C. elegans* VRK-1 phosphorylated AAK-2 isoform b at Thr$^{243}$, an equivalent residue for Thr$^{172}$ in the mammalian AMPK (Fig. 6H). We also found that the *aak-2(T181A)::GFP*, which alters the Thr$^{181}$ to Ala in the isoform c, homologous to Thr$^{172}$ to Ala change in the mammalian AMPK, did not restore the longevity of *vrk-1::GFP O/E* in an *aak-2(−)* mutant background (fig. S9, E and F). Thus, *C. elegans* VRK-1 appears to phosphorylate AAK-2 for life span extension. Last, we demonstrated that *vrk-1* overexpression in *C. elegans* increased the level of active p-AMPK (Fig. 6I and fig. S8K). Conversely, genetic inhibition of *vrk-1* by RNAi or by a reduction of function mutation, *vrk-1(x1)*, decreased p-AMPK levels that were elevated by *isp-1* mutations (Fig. 6I and fig. S8K). These data suggest that VRK-1/VRK1 functions as an upstream kinase of AMPK. Together, VRK1 functions to increase the activity of life span–extending AMPK via phosphorylation in an evolutionarily conserved manner.

## DISCUSSION

### Somatic nuclear expression of *vrk-1* increases life span by activating AMPK through phosphorylation in *C. elegans*

The evolutionarily conserved protein kinase, VRK-1, has been known to function in cell division in *C. elegans*. However, its role in postmitotic somatic cells has remained elusive. Here, we showed that *vrk-1* was highly expressed in various somatic tissues in adult *C. elegans*. Moreover, VRK-1 was essential and sufficient for the longevity of adult *C. elegans*. We further found that VRK-1 extended life span by increasing the level of active AMPK through phosphorylation. We demonstrated that both *C. elegans* VRK-1 and human VRK1 activated AMPK via direct phosphorylation. Thus, our data provide mechanisms by which VRK-1, a nuclear protein kinase known to regulate cell division, promotes longevity by functioning in postmitotic somatic cells.

### Expression of *vrk-1* in the soma of adult animals is critical for life span extension

Previous reports have revealed that *vrk-1* is required for germ cell proliferation and proper cell division. In this study, we show that *vrk-1* also functions in postmitotic somatic cells to promote organismal longevity. Several cell cycle–regulatory or DNA damage checkpoint proteins play additional roles in postmitotic somatic cells of *C. elegans*. For example, genetic inhibition of the cell cycle checkpoint genes, caffeine-induced death 1 (*cid-1*), checkpoint kinase 1 (*chk-1*), and cell division cycle 25.1 (*cdc-25.1*), increases endoplasmic reticulum protein homeostasis in postmitotic cells and increases life span, thus indicating postmitotic functions for these cell cycle regulators (*27*). Similarly, knockdown of *cyclin E* (*cye-1*) or cyclin-dependent kinase 2 (*cdk-2*) increases the life span of adult *C. elegans* and enhances stress resistance (*28*). Our data indicate that VRK-1 also plays key roles in the soma of adult animals in addition to regulating germ cell division in developing larvae.

### VRK-1 is an AMPK-activating kinase acting in the nucleus

AMPK and its upstream regulators have been extensively studied as key factors that control cell metabolism. LKB1 and CaMKKβ, two established AMPK upstream kinases, directly phosphorylate AMPK via distinct signaling pathways. LKB1 is considered to be constitutively active and phosphorylates AMPK, whereas CaMKKβ phosphorylates AMPK when $Ca^{2+}$ levels are increased [reviewed in (*9*)]. TAK1 may also function as an AMPK upstream kinase [reviewed in (*9*, *29*)]. In our current work, we identified VRK1 as a novel upstream activating kinase of AMPK and further demonstrated the physiological importance of VRK-1–to–AMPK signaling for organismal longevity. Our data indicate that VRK-1 mediates the activation and the phosphorylation of AMPK upon inhibition of mitochondrial respiration. Therefore, we speculate that the increased AMP/ADP-to-ATP ratio resulting from impaired mitochondrial respiration enhances VRK-1–mediated phosphorylation of AMPK to promote longevity in *C. elegans*. In future studies, it will be important to further dissect the molecular mechanisms by which VRK-1 phosphorylates AMPK under mitochondria-defective conditions in both *C. elegans* and mammals.

We also propose that VRK-1 has functions that are distinct from other known AMPK kinases, mainly because of the fact that VRK-1 is a nuclear kinase, whereas LKB1 and CaMKKβ function in the cytoplasm. In *C. elegans*, AMPK is mostly localized in the nucleus (*26*). Mammalian AMPKα2 is also preferentially localized to the nucleus (*30*), and AMPKα1 displays circadian rhythm–dependent nuclear localization in mice (*31*). Therefore, our study proposes a possibility that the nuclear kinase, VRK-1, may phosphorylate AMPKα1 and/or AMPKα2 in the nucleus and thus contribute to the transcriptional changes elicited by factors acting downstream of AMPK.

### Mammalian VRKs may play beneficial roles in animal physiology, including longevity

In mammals, VRK1 plays pivotal roles in various biological processes, and loss of VRK1 function leads to severe defects. Life span is often associated with telomere length in various organisms, including humans (*32*, *33*). Mouse VRK1 phosphorylates and activates heterogeneous nuclear ribonucleoprotein A1, a single-stranded oligonucleotide-binding protein that plays an important role in telomere maintenance (*34*). Loss-of-function *VRK1* mutant mice exhibit shortening of telomeres in male germ cells (*34*). In addition, the genetic inhibition of *VRK1* results in defective cell proliferation, whereas overexpression of *VRK1* stabilizes p53 and increases its transcriptional activity (*35*). These findings suggest that VRK1 plays an integral role in maintaining normal cellular function and physiology in animals.

The functions and phosphorylation targets of VRKs are highly conserved across species. Genetic and/or biochemical interaction between VRK-1 and its targets, BAF-1 and p53, has been shown in both mammalian cells and *C. elegans*, suggesting that these organisms share other common targets of VRK-1 (*14*–*16*, *35*, *36*). In particular, mutations in *BAF* result in aberrant nuclear envelope structure and are associated with progeria syndrome in humans (*37*). It is therefore tempting to speculate that the loss of *VRK1* may lead to impairment in BAF function, which disrupts its interaction with LEM (LAP2, emerin, and MAN1) domain proteins and triggers progeria-like phenotypes. In our study, we demonstrated that VRK-1 activated AMPK by phosphorylation to extend life span in *C. elegans*. Considering the conserved role of reduced mitochondrial respiration in life span, it will not be surprising to find that VRK1

also contributes to longevity in mammals, likely through activation of AMPK.

## MATERIALS AND METHODS

### Strains

Worms were grown on *Escherichia coli* OP50-seeded plates following standard laboratory culture conditions. Some of the strains used in this study were obtained from Caenorhabditis Genetics Center, which is funded by the National Institutes of Health (NIH) Office of Research Infrastructure (P40 OD010440). The *C. elegans* strains used in this study are as follows: wild-type Bristol strain N2, IJ848 *yhEx432[vrk-1p::vrk-1::gfp; odr-1p::rfp]*, IJ849 *yhEx433[vrk-1p::vrk-1::gfp; odr-1p::rfp]*, IJ288 *yhEx63[vrk-1p::vrk-1::gfp; rol-6D]*, IJ289 *yhEx534 [vrk-1p::vrk-1::gfp; rol-6D]*, CF1290 N2 carrying pRF4(*rol-6(su1006)*) marker, YL279 *unc-119(ed3); vrIs18[pie-1p::gfp:vrk-1:pie-1 3′UTR; unc-119(+)]*, IJ391 *vrk-1(x1) II*, CF2172 *isp-1(qm150) IV*, CF2354 *clk-1(qm30) III*, IJ401 *vrk-1(x1) II; clk-1(qm30) III*, IJ402 *vrk-1(x1) II; isp-1(qm150) IV*, CF1041 *daf-2(e1370) III*, IJ173 *eat-2(ad1116) II*, CF2553 *osm-5(p813) X*, IJ7 *vhl-1(ok161) X*, IJ1376 *vrk-1(x1) eat-2(ad1116) II*, IJ1377 *vrk-1(x1) II; daf-2(e1370) III*, IJ1378 *vrk-1(x1) II; osm-5(p813) X*, IJ32 *Iszc[hsp-6p::gfp]*, IJ31 *isp-1(qm150) IV; Iszc [hsp-6p::gfp]*, ZG120 *iaIs7[nhr-57p::GFP; unc-119(+)]*, IJ2 *isp-1(qm150) IV; iaIs7[nhr-57p::GFP; unc-119(+)]*, CL2166 *dvIs19[pAF15(gst-4::GFP::NLS)]*, IJ945 *isp-1(qm150) IV; dvIs19[pAF15(gst-4::GFP::NLS)]*, IJ1670 *yhIs90 [vrk-1p::vrk-1::GFP; odr-1p::RFP]*, IJ1721 *aak-2(ok524) IV; yhIs90 [vrk-1p::vrk-1::GFP; odr-1p::RFP]*, CF2725 *aak-2(ok524) X*, IJ259 *isp-1 (qm150) IV; aak-2(ok524) X*, AGD418 *uthIs205[crtc-1p::crtc-1::RFP:: unc-54 3′UTR; rol-6D]*, IJ1945 *uthIs205[crtc-1p::crtc-1::RFP::unc-54 3′UTR; rol-6D]; yhIs90[vrk-1p::vrk-1cDNA::GFP; odr-1p::RFP]*, *IJ249 yhEx53[aak-2p::aak-2(T181A)::GFP; rol-6D]*, IJ1942 *aak-2(ok524) X; yhEx53[aak-2p::aak-2(T181A)::GFP; rol-6D]*, IJ1943 *aak-2(ok524) X; yhIs90[vrk-1p::vrk-1cDNA::GFP; odr-1p::RFP]; yhEx53[aak-2p::aak-2 (T181A)::GFP; rol-6D]*, IJ2017 *vrk-1(ok1181)/mIn1[mIs14 dpy-10(e128)]*, IJ2018 *vrk-1(ok1181)/mIn1[mIs14 dpy-10(e128)]; daf-2(e1370)*, and IJ2019 *vrk-1(ok1181)/mIn1[mIs14 dpy-10(e128)]; isp-1(qm150)*.

### Life-span analysis

Life-span assays were conducted at 20°C on nematode growth medium (NGM) plates seeded with *E. coli* OP50 or HT115 for RNAi experiments, starting at day 1 of adulthood. Worm strains that were used for experiments were kept at 20°C for at least three generations before life-span assays. Briefly, gravid adult worms were allowed to lay eggs on plates seeded with OP50 or HT115, and the worms that developed to prefertile young adults were transferred to new plates. For life-span assays without chemical 5-fluoro-2′-deoxyuridine (FUDR), which prevents progeny from hatching, young adults were placed on new plates every 1 or 2 days until they ceased to lay eggs. For life-span assays with FUDR, synchronized young adult worms were transferred to new plates containing FUDR (5 μM; Sigma-Aldrich, MO, USA). For RNAi experiments, 1 mM isopropyl-thiogalactoside (Gold Biotechnology, St. Louis, MO, USA) was added to plates seeded with HT115 that express specific double-stranded RNA (dsRNA) and incubated at room temperature for ~24 hours. For double RNAi experiment, HT115 RNAi bacteria were grown in liquid LB media containing ampicillin (50 μg/ml; USB, Santa Clara, CA, USA) until the media display the optical density measured at a wavelength 600 nm of 0.9. Two different HT115 targeting different genes were mixed at the ratio 1:1 for double RNAi. HT115 that express an empty RNAi plasmid (L4440) were mixed with specific RNAi bacteria for control. For all the life-span assays, a minimum of five plates with worms were used for each condition except for the ones that included discarded plates due to contamination. All the life-span assays were conducted by at least two independent researchers at least twice per condition. All the mutant animals that were used for life-span assays were outcrossed to Lee laboratory wild-type N2 at least three times before the experiments. Animals that displayed internal hatching or ruptured vulvae or crawled off the plates were censored but included in the life-span analysis as censored worms. Online application for the survival analysis 2 (http://sbi.postech.ac.kr/oasis2) was used for statistical analysis of the data, and *P* values were calculated using the log-rank (Mantel-Cox) test.

### DNA staining with 4′,6-diamidino-2-phenylindole

Stage-synchronized worms were harvested with M9 buffer with polyethylene glycol 4000 (PEG 4000) (0.01%; Tokyo Chemical Industry, Japan) and washed three times with M9 buffer. Worms were fixed with 4% paraformaldehyde (158127, Sigma-Aldrich, MO, USA) solution in phosphate-buffered saline (PBS) (137 mM NaCl, 2.7 mM KCl, 8 mM $Na_2HPO_4$, and 2 mM $KH_2PO_4$; AM9624, Thermo Fisher Scientific, MA, USA) for 45 min with gentle agitation. After fixation, worms were washed with PBS containing 0.01% PEG 4000 twice with gentle agitation for 5 min for each washing step. Fixed worms were stored in 70% ethanol at 4°C overnight. Worms were placed on a 2% agarose pad on a slide glass, and the worms were soaked in a drop of 4′,6-diamidino-2-phenylindole (DAPI) solution (2 ng/μl) (62248, Thermo Fisher Scientific, MA, USA) in VECTASHIELD antifade mounting media (Vector Laboratories, CA, USA). After covering the agar pad with a coverslip, worms were incubated for at least 30 min in the dark before imaging.

### Microscopy and quantification of fluorescence

Confocal fluorescence images of VRK-1::GFP and CRTC-1::RFP were acquired using an inverted LSM 880 laser scanning microscope (Zeiss Corporation, Germany) with Plan-Apochromat 20× 0.8 M27, C-Apochromat 40× 1.2 water Korr FCS M27, or Plan-Apochromat 63× 1.4 oil differential interference contrast (DIC) M27 objectives. Green fluorescence was detected under the excitation wavelength at 488 nm and emission wavelength at 526 nm. Red fluorescence was detected under the excitation wavelength at 561 nm and emission wavelength at 668 nm. DAPI signal was detected under the excitation wavelength at 405 nm and emission wavelength at 498 nm. Confocal *Z* stack fluorescence images shown in Fig. 1B were acquired using an inverted Leica (Wetzlar, Germany) TCS SP8 laser scanning confocal microscope with a 40× 1.3 numerical aperture oil or 63× 1.2 water objective. Green fluorescence was detected under the excitation wavelength at 488 nm and emission wavelength at 520 nm. Microphotographs used in Fig. 1B were obtained using Z-project (average intensity) function in ImageJ software (Rasband, W. S., ImageJ, U.S. NIH, Bethesda, MD, USA; http://rsbweb.nih.gov/ij/, 1997–2018). Fluorescence images of animals expressing *hsp-6p::GFP*, *nhr-57p::GFP*, or *gst-4p::GFP* were captured by using Axiocam (Zeiss Corporation, Germany) mounted to a HRc Zeiss Axioscope A.1 (Zeiss Corporation, Germany) equipped with EC Plan-Neofluar (Zeiss Corporation, Germany) objective lens. Green fluorescence was detected under Zeiss filter set 38 HE emission filter (Zeiss Corporation, Germany). Fluorescence images of CRTC-1::RFP used for quantification shown in Fig. 5E were

captured by two researchers independently, using DS-Qi1Mc (Nikon, Japan) mounted on Nikon ECLIPSE Ni microscope (Nikon, Japan) with Plan Fluor 40× DIC M N2 objective (Nikon, Japan) and NEO scientific complementary metal-oxide semiconductor camera (Andor, Belfast, UK) mounted on Nikon Eclipse Ti2 inverted confocal microscope (Nikon, Japan) with a Niji light-emitting diode light source (Bluebox Optics, Huntingdon, UK) and a 10× objective (Nikon, Japan); the red fluorescence was detected under tetramethyl rhodamine isothiocyanate (TRITC) band-pass filter (Nikon, Japan) in the Eclipse Ni and ET-DsRed (TRITC/Cy3) filter (Chroma Technology, VT, USA) in the Eclipse Ti2 microscopes, respectively. Image planes that showed distinct nuclear morphology assessed by DAPI signals were chosen for imaging in Figs. 1A and 5D and figs. S1, S6J, and S7B. Image planes that showed distinct foci on nuclei with green fluorescence in the intestine for Fig. 1B were chosen. Image planes were chosen for the regions where outlines of most worms were visible for fig. S5 (C to E). ImageJ software was used to quantify GFP intensity with arbitrary unit by measuring average pixel intensity. Fluorescence intensity of individual worms was normalized by subtracting background signals, and mean fluorescence intensity was calculated by averaging the normalized values of >60 individuals. Levamisole (2 mM) was used to immobilize the animals on 2% agarose pads before imaging. *P* values were calculated using the unpaired Student's *t* test (two-tailed) by comparing mean fluorescence intensity of experimental group with that of control group.

### qRT-PCR analysis

Synchronized L4 or young adult animals grown at 20°C were used for RNA extraction, cDNA synthesis, and qRT-PCR analysis. For qRT-PCR analysis of food-deprived animals shown in fig. S7A, day 3 adult worms were used. Briefly, RNAiso (Takara, Japan) was used to extract total RNA, and cDNA was obtained using ImProm-II Reverse Transcriptase (Promega, WI, USA). A 7300 Real-Time PCR System (Applied Biosystems) was used to perform quantitative PCR experiments, and the results were analyzed by using the comparative $C_T$ method described in the manufacturer's manual. The average values of the mRNA levels of *ama-1*, *tba-1*, or *pmp-3* gene were used for normalization. The average of at least two technical repeats was applied for each biological data point.

### Food deprivation of *C. elegans*

For qRT-PCR analysis of food-deprived worms, wild-type embryos were obtained by using a bleaching method (*7*) and placed on control RNAi or *vrk-1* RNAi bacteria-seeded NGM plates. Worms were then grown until reaching day 2 adults, harvested with M9 buffer, and washed three times to remove remaining bacteria. For a fed condition, worms were placed on control RNAi bacteria– or *vrk-1* RNAi bacteria–seeded NGM plates. For a food deprivation condition, worms were placed on NGM plates containing streptomycin (10 μg/ml) to prevent *E. coli* (HT115) that expresses dsRNA from growth, harvested with M9 buffer, and used for RNA extraction and qRT-PCR analysis after 24 hours of food deprivation. FUDR was applied to prevent progeny from hatching at L4 stage. For assaying the subcellular localization of CRTC-1::RFP, worms were treated with control RNAi from hatching until they reached L2 or L3 stages. The animals were then collected with M9 buffer, washed three times, and placed on NGM plates containing streptomycin (50 μg/ml) and kanamycin (50 μg/ml) for food deprivation. After 24 hours of food deprivation, the worms were used for micrograph imaging.

### In vitro kinase assay

Recombinant His-VRK1, GST-AMPKα2, GST–AMPKα2-KD (K45R), His-VRK-1, GST–AAK-2 isoform b, and GST–AAK-2 isoform b-KD (K116R) proteins were expressed in *E. coli* BL21 (DE3). GST-AMPKα2 and GST–AAK-2 were purified using glutathione Sepharose 4B (GE Healthcare Life Sciences, MA, USA). His-VRK1 and His-VRK-1 were purified with Ni–nitrilotriacetic acid agarose (Invitrogen, CA, USA) following the manufacturers' instructions. For nonradioactive in vitro kinase assays using human VRK1 and AMPK, purified His-VRK1 was incubated with recombinant GST-AMPKα2 in the kinase assay buffer [60 mM HEPES (pH 7.4), 10 mM $MgCl_2$, and 10 mM $MnCl_2$] and 200 μM ATP for 30 min at 30°C. The enzyme reaction was stopped by the addition of 5× SDS loading buffer by boiling at 95°C for 5 min. Samples were immunoblotted with antibodies against GST (91G1, Cell Signaling Technology, MA, USA), His (2365S, Cell Signaling Technology, MA, USA), or p-AMPKα (Thr$^{172}$) (2531S, Cell Signaling Technology, MA, USA). The nonradioactive in vitro kinase assays for *C. elegans* VRK-1 and AAK-2 was performed similarly to those for the human VRK1 and AMPK. For radioactive in vitro kinase assay, purified His-VRK1 was incubated with recombinant GST-AMPKα2 in kinase assay buffer [60 mM HEPES (pH 7.4), 10 mM $MgCl_2$, and 10 mM $MnCl_2$] and [γ-$^{32}$P]ATP for 30 min at 30°C. The reaction was stopped by the addition of 5× SDS loading buffer by boiling at 95°C for 5 min. Radioactive signal was detected by using an x-ray film (Agfa, Antwerp, Belgium).

### Immunoprecipitation

For immunoprecipitation of endogenous AMPK, human embryonic kidney (HEK) 293A cells were resuspended with cell lysis buffer [20 mM Tris, 150 mM NaCl, 1 mM EDTA, 0.5% Triton X-100, and protease inhibitor cocktail (F. Hoffmann–La Roche, Basel, Switzerland)] and disrupted by using sonication. One milligram of cell lysates was incubated with Protein A agarose bead (F. Hoffmann–La Roche, Basel, Switzerland) and normal rabbit immunoglobulin G (IgG; 2729S, Cell Signaling Technology, MA, USA) or anti-AMPK antibody (2532S, Cell Signaling Technology, MA, USA) overnight at 4°C on a rotator. After incubation, beads were washed four times with cell lysis buffer. Bound proteins were eluted with 2× SDS sample buffer and 10 mM dithiothreitol. Immunoprecipitated proteins were analyzed by immunoblotting. VeriBlot for IP Detection Reagent (AB131366, Abcam, Cambridge, UK) was used to detect the VRK1 band without interference from IgG heavy chain. Immunoprecipitation experiments using overexpression of Flag-AMPK and/or hemagglutinin (HA)–VRK1 was performed using $3 \times 10^6$ HEK293A cells in cell lysis buffer [50 mM Tris (pH 7.5), 150 mM NaCl, 1 mM EDTA, and 1% Triton X-100] supplemented with protease inhibitors (A32953, Thermo Fisher Scientific, MA, USA). Cell lysates were incubated overnight with an anti-Flag antibody (F1804, Sigma-Aldrich, MO, USA) and protein G Sepharose beads (GE Healthcare Life Sciences, MA, USA) at 4°C on a rotator. After incubation, the beads were washed three times with the cell lysis buffer and boiled for 5 min at 95°C. Samples were immunoblotted with antibodies against Flag (2368S, Cell Signaling Technology, MA, USA), VRK1 (*38*), p-AMPKα (Thr$^{172}$) (2531S, Cell Signaling Technology, MA, USA), HA (A190-108A, Bethyl Laboratories, TX, USA), or glyceraldehyde-3-phosphate dehydrogenase (GAPDH) (sc-47724, Santa Cruz Biotechnology, TX, USA).

### Western blot analysis

Western blot analysis using *C. elegans* samples was performed with synchronized L4 or young adult animals, which were harvested, washed three times using M9 buffer, and centrifuged at 1400 rpm for 30 s. The worms were shock-frozen in liquid nitrogen, mixed with SDS sample buffer, and boiled for 10 min. The samples were subsequently vortexed for 10 min and centrifuged for 30 min at 15,700*g* at 4°C, and the supernatant was collected. The worm protein samples were electrophoresed using 8% SDS–polyacrylamide gel electrophoresis and transferred to polyvinylidene difluoride membrane. The membrane was blocked with TBS-T [20 mM Tris-HCl (pH 7.6), 140 mM NaCl, and 0.1% Tween 20] buffer containing 5% bovine serum albumin for 1 hour at room temperature and incubated with primary antibodies against p-AMPKα (1:2000; 2531S, Cell Signaling Technology, MA, USA) or α-tubulin (1:1000; sc-32293, Santa Cruz Biotechnology, TX, USA) overnight at 4°C. Anti-rabbit (1:15,000; Thermo Fisher Scientific, MA, USA) or anti-mouse (1:5000; Thermo Fisher Scientific, MA, USA) secondary antibodies conjugated with horseradish peroxidase were used to detect anti-AMPKα or anti–α-tubulin primary antibodies, respectively. The membrane was incubated in the chemiluminescent horseradish peroxidase substrate (Thermo Fisher Scientific, MA, USA), and the signal was detected by using x-ray film (Agfa, Antwerp, Belgium). Western blot analysis using cultured human cells was performed as previously described (*38*). Western blot data were quantified using ImageJ software.

### Generation of transgenic animals

To generate transgenic animals expressing GFP-fused VRK-1, a promoter (~1 kb) and the genomic region of *vrk-1* (~2.5 kb) were PCR-amplified from *C. elegans* genomic DNA. The PCR products were fused to Gateway donor vectors using BP Clonase (Invitrogen) followed by recombination with a Gateway destination vector containing *GFP* and *unc-54* 3′UTR using LR Clonase (Invitrogen). *vrk-1p::vrk-1::gfp* expression vector (25 ng/μl) was coinjected with an injection marker *odr-1p::rfp* (75 ng/μl) or pRF4(*rol-6(su1006)*) (75 ng/μl) into the gonad of day 1 adult wild-type animals. Transgenic animals expressing T181A mutant AAK-2 were generated by microinjection of PWM23 *aak-2(T181A)::GFP* expression vector (a gift from W. B. Mair) (25 ng/μl) and pRF4(*rol-6(su1006)*) (75 ng/μl).

### mRNA library preparation and sequencing

Wild-type N2 and *isp-1(qm150)* mutant animals were synchronized by using an embryo bleaching method (*7*), and synchronized larvae were fed with either control or *vrk-1* RNAi bacteria until the worms reached young adult stage. Worms were harvested with M9 buffer, washed to remove remaining bacteria, and frozen in liquid nitrogen. Three independent biological repeats for each condition were used for mRNA-seq experiments. Total RNAs were isolated using RNAiso plus (Takara, Shiga, Japan), followed by ethanol precipitation. Paired-end mRNA-seq library was prepared and sequenced by Illumina platform at Macrogen (Macrogen Inc., Seoul, South Korea).

### mRNA-seq analysis

Reads were aligned to the *C. elegans* genome ce11 (Ensembl WBcel235.87) by HISAT2 (version 2.0.5) with default parameters. Aligned reads were assembled to transcripts and levels of these transcripts were quantified by using SeqMonk (www.bioinformatics.babraham.ac.uk/projects/seqmonk/). FPKM (fragments per kilobase of transcript per million mapped reads) values were calculated by using RNA-seq. Quantitation pipeline and *P* values were calculated using EdgeR. Protein-coding genes whose FPKM values in wild type treated with control RNAi were greater than 1 were used for DEG analysis. Overlapping genes between our mRNA-seq data and published transcriptome data were analyzed by using WormExp (version 1.0). Venn diagrams were made by using Venn Diagram Plotter (http://omics.pnl.gov/software/venn-diagram-plotter), and representation factors for overlaps between two different gene sets were calculated (http://nemates.org/MA/progs/overlap_stats.html).

### GO analysis

GO analysis for genes up- or down-regulated by *isp-1* mutations in a *vrk-1*–dependent manner was performed by using DAVID. Enriched biological process GO terms with $P < 0.05$ and false discovery rate < 0.05 were listed.

### Primers used for cloning

***vrk-1 promoter Gateway***

Forward: GGGGACAACTTTGTATAGAAAAGTTGAAATCGCGAATCAAGAAA

Reverse: GGGGACTGCTTTTTTGTACAAACTTGTCATTCTACCTGAAAATGAAA

***vrk-1 coding region Gateway***

Forward: GGGGACAAGTTTGTACAAAAAAGCAGGCTTGCCACCGAAAAAAGCTCCCGCCAAAA

Reverse: GGGGACCACTTTGTACAAGAAAGCTGGGTACACTTCCGACGAGCAGCTCGAAT

### siRNA

Scrambled siRNA: CCUACGCCACCAAUUUCGU(dTdT)

*VRK1* siRNA: CAAGGAACCTGGTGTTGAA(dTdT)

### qRT-PCR primers

***ama-1***

Forward: TGGAACTCTGGAGTCACACC

Reverse: CATCCTCCTTCATTGAACGG

***tba-1***

Forward: GTACACTCCACTGATCTCTGCTGACAAG

Reverse: CTCTGTACAAGAGGCAAACAGCCATG

***pmp-3***

Forward: GTTCCCGTGTTCATCACTCAT

Reverse: ACACCGTCGAGAAGCTGTAGA

***vrk-1***

Forward: GCCATGGATGGCTCTCGAATCGT

Reverse: CTGGATTGCCAGGCACCTTGC

***vrk-1-3′UTR***

Forward: GATGATTATCAAAGAGACCAG

Reverse: GGGATGCAATGTGACTCG

***cco-1***

Forward: TTGCTGGAGATGATCGTTAC

Reverse: CATCCAATGATTCTGAAGTCG

***ceh-23***

Forward: CAATTCCAGCACAGCCTTTTATTCC

Reverse: GCATTTGCAAGAGCTTCGACAGC

***col-176***

Forward: CAGCTGGACAACCAGGAAC

Reverse: GTCCTGGAGCACACTTGATG

***col-90***
Forward: ACACCAGGATCAAATGGAAG
Reverse: TAGTTGGCGTCTTTTCCAAC
***rol-6***
Forward: AATCGCCAACTTCAGAAGTC
Reverse: TATTGTTGACGTCTCACACG
***R11G11.6***
Forward: CAGACCAATAATCTTTCGGATC
Reverse: AACTGAAGATAGTTGGGAGATG
***col-17***
Forward: GTTTGCTTCTTATTTTGGGTAC
Reverse: TGCGAGGTGTCTGAGATG
***bli-2***
Forward: ATGGACGAGAAGGAACTGAA
Reverse: AAGTTGATACTGTGCTGATG
***dpy-10***
Forward: TGTGTTGCTCTCCCAATTATG
Reverse: CCTCGTCGTTTGATCTTTCG
***col-73***
Forward: AGAGCCAGGACAAGATGGAG
Reverse: AGTGATCGCATCCTCCCTTG
***E01G4.6***
Forward: GCTCGATTTCCCATCATGAG
Reverse: CGAGCAGTTGTTTGAGTGTG
***col-14***
Forward: CTTGGAGAGTGTCACGTTTC
Reverse: TGTTGGATATTGAAACTGGAGG
***F35B3.4***
Forward: TCAATACTGTGCTGCTCAAG
Reverse: CGCAGAAAGTGAAGCATTTG
***Y47D7A.13***
Forward: GACAAGGATACCAACAACAGC
Reverse: TCTCCGTATGAGGCAGCTG
***wrt-6***
Forward: GTACTAGATCCGACTTAAAATTG
Reverse: TTCTTGATGACGACATTGCTG
***Y11D7A.9***
Forward: TTACGGAAATTGTCAGGCTG
Reverse: TATGGAATATTAGGGCAATTGC
***tax-6***
Forward: TGTGGGAGAAAAAGTAACGG
Reverse: TCAAAGGTGTCATCGCATTC
***par-5***
Forward: CGCCATGAAGAAAGTGACC
Reverse: GAACGGCGAGCTCCGAC
***ftt-2***
Forward: GACCTCGGACGCTGCC
Reverse: GTAACGTGTCGGTGTGAAG

## SUPPLEMENTARY MATERIALS

Supplementary material for this article is available at http://advances.sciencemag.org/cgi/content/full/6/27/eaaw7824/DC1

View/request a protocol for this paper from *Bio-protocol*.

## REFERENCES AND NOTES


1. D. C. Wallace, R. J. Youle, *Mitochondria* (Cold Spring Harbor Laboratory Press, 2014).
2. H. D. Osiewacz, *The Mitochondrion in Aging and Disease* (Academic Press, 2014).
3. Y. Wang, S. Hekimi, Mitochondrial dysfunction and longevity in animals: Untangling the knot. *Science* **350**, 1204–1207 (2015).
4. A. Salminen, K. Kaarniranta, AMP-activated protein kinase (AMPK) controls the aging process via an integrated signaling network. *Ageing Res. Rev.* **11**, 230–241 (2012).
5. H.-W. Chang, S. Pisano, A. Chaturbedi, J. Chen, S. Gordon, A. Baruah, S. S. Lee, Transcription factors CEP-1/p53 and CEH-23 collaborate with AAK-2/AMPK to modulate longevity in *Caenorhabditis elegans*. *Aging Cell* **16**, 814–824 (2017).
6. R. Curtis, G. O'Connor, P. S. DiStefano, Aging networks in *Caenorhabditis elegans*: AMP-activated protein kinase (*aak-2*) links multiple aging and metabolism pathways. *Aging Cell* **5**, 119–126 (2006).
7. A. B. Hwang, E.-A. Ryu, M. Artan, H.-W. Chang, M. H. Kabir, H.-J. Nam, D. Lee, J.-S. Yang, S. Kim, W. B. Mair, C. Lee, S. S. Lee, S.-J. Lee, Feedback regulation via AMPK and HIF-1 mediates ROS-dependent longevity in *Caenorhabditis elegans*. *Proc. Natl. Acad. Sci. U.S.A.* **111**, E4458–E4467 (2014).
8. S. Herzig, R. J. Shaw, AMPK: Guardian of metabolism and mitochondrial homeostasis. *Nat. Rev. Mol. Cell Biol.* **19**, 121–135 (2018).
9. D. Carling, M. J. Sanders, A. Woods, The regulation of AMP-activated protein kinase by upstream kinases. *Int. J. Obes.* **32**, S55–S59 (2008).
10. G. Manning, D. B. Whyte, R. Martinez, T. Hunter, S. Sudarsanam, The protein kinase complement of the human genome. *Science* **298**, 1912–1934 (2002).
11. J. Nezu, A. Oku, M. H. Jones, M. Shimane, Identification of two novel human putative serine/threonine kinases, VRK1 and VRK2, with structural similarity to vaccinia virus B1R kinase. *Genomics* **45**, 327–331 (1997).
12. I. Zelko, R. Kobayashi, P. Honkakoski, M. Negishi, Molecular cloning and characterization of a novel nuclear protein kinase in mice. *Arch. Biochem. Biophys.* **352**, 31–36 (1998).
13. A. Valbuena, M. Sanz-García, I. López-Sánchez, F. M. Vega, P. A. Lazo, Roles of VRK1 as a new player in the control of biological processes required for cell division. *Cell. Signal.* **23**, 1267–1272 (2011).
14. C. Asencio, I. F. Davidson, R. Santarella-Mellwig, T. B. Ly-Hartig, M. Mall, M. R. Wallenfang, I. W. Mattaj, M. Gorjánácz, Coordination of kinase and phosphatase activities by Lem4 enables nuclear envelope reassembly during mitosis. *Cell* **150**, 122–135 (2012).
15. M. Gorjánácz, E. P. F. Klerkx, V. Galy, R. Santarella, C. López-Iglesias, P. Askjaer, I. W. Mattaj, *Caenorhabditis elegans* BAF-1 and its kinase VRK-1 participate directly in post-mitotic nuclear envelope assembly. *EMBO J.* **26**, 132–143 (2007).
16. K. Waters, A. Z. Yang, V. Reinke, Genome-wide analysis of germ cell proliferation in *C. elegans* identifies VRK-1 as a key regulator of CEP-1/p53. *Dev. Biol.* **344**, 1011–1025 (2010).
17. A. Dobrzynska, P. Askjaer, Vaccinia-related kinase 1 is required for early uterine development in *Caenorhabditis elegans*. *Dev. Biol.* **411**, 246–256 (2016).
18. E. P. F. Klerkx, P. Alarcón, K. Waters, V. Reinke, P. W. Sternberg, P. Askjaer, Protein kinase VRK-1 regulates cell invasion and EGL-17/FGF signaling in *Caenorhabditis elegans*. *Dev. Biol.* **335**, 12–21 (2009).
19. W. G. Kelly, S. Xu, M. K. Montgomery, A. Fire, Distinct requirements for somatic and germline expression of a generally expressed *Caernorhabditis elegans* gene. *Genetics* **146**, 227–238 (1997).
20. W. Yang, K. Dierking, H. Schulenburg, WormExp: A web-based application for a *Caenorhabditis elegans*-specific gene expression enrichment analysis. *Bioinformatics* **32**, 943–945 (2016).
21. D. Cristina, M. Cary, A. Lunceford, C. Clarke, C. Kenyon, A regulated response to impaired respiration slows behavioral rates and increases lifespan in *Caenorhabditis elegans*. *PLOS Genet.* **5**, e1000450 (2009).
22. M. J. Falk, Z. Zhang, J. R. Rosenjack, I. Nissim, E. Daikhin, I. Nissim, M. M. Sedensky, M. Yudkoff, P. G. Morgan, Metabolic pathway profiling of mitochondrial respiratory chain mutants in *C. elegans*. *Mol. Genet. Metab.* **93**, 388–397 (2008).
23. C. Yee, W. Yang, S. Hekimi, The intrinsic apoptosis pathway mediates the pro-longevity response to mitochondrial ROS in *C. elegans*. *Cell* **157**, 897–909 (2014).
24. K. Burkewitz, I. Morantte, H. J. M. Weir, R. Yeo, Y. Zhang, F. K. Huynh, O. R. Ilkayeva, M. D. Hirschey, A. R. Grant, W. B. Mair, Neuronal CRTC-1 governs systemic mitochondrial metabolism and lifespan via a catecholamine signal. *Cell* **160**, 842–855 (2015).
25. L. Hou, D. Wang, D. Chen, Y. Liu, Y. Zhang, H. Cheng, C. Xu, N. Sun, J. McDermott, W. B. Mair, J.-D. J. Han, A systems approach to reverse engineer lifespan extension by dietary restriction. *Cell Metab.* **23**, 529–540 (2016).
26. W. Mair, I. Morantte, A. P. C. Rodrigues, G. Manning, M. Montminy, R. J. Shaw, A. Dillin, Lifespan extension induced by AMPK and calcineurin is mediated by CRTC-1 and CREB. *Nature* **470**, 404–408 (2011).
27. A. Olsen, M. C. Vantipalli, G. J. Lithgow, Checkpoint proteins control survival of the postmitotic cells in *Caenorhabditis elegans*. *Science* **312**, 1381–1385 (2006).
28. M. Dottermusch, T. Lakner, T. Peyman, M. Klein, G. Walz, E. Neumann-Haefelin, Cell cycle controls stress response and longevity in *C. elegans*. *Aging* **8**, 2100–2126 (2016).
29. D. Neumann, Is TAK1 a direct upstream kinase of AMPK? *Int. J. Mol. Sci.* **19**, 2412 (2018).

30. I. Salt, J. W. Celler, S. A. Hawley, A. Prescott, A. Woods, D. Carling, D. G. Hardie, AMP-activated protein kinase: Greater AMP dependence, and preferential nuclear localization, of complexes containing the α2 isoform. *Biochem. J.* **334**, 177–187 (1998).
31. K. A. Lamia, U. M. Sachdeva, L. DiTacchio, E. C. Williams, J. G. Alvarez, D. F. Egan, D. S. Vasquez, H. Juguilon, S. Panda, R. J. Shaw, C. B. Thompson, R. M. Evans, AMPK regulates the circadian clock by cryptochrome phosphorylation and degradation. *Science* **326**, 437–440 (2009).
32. B. J. Heidinger, J. D. Blount, W. Boner, K. Griffiths, N. B. Metcalfe, P. Monaghan, Telomere length in early life predicts lifespan. *Proc. Natl. Acad. Sci. U.S.A.* **109**, 1743–1748 (2012).
33. T. Steenstrup, J. D. Kark, S. Verhulst, M. Thinggaard, J. V. B. Hjelmborg, C. Dalgård, K. O. Kyvik, L. Christiansen, M. Mangino, T. D. Spector, I. Petersen, M. Kimura, A. Benetos, C. Labat, R. Sinnreich, S.-J. Hwang, D. Levy, S. C. Hunt, A. L. Fitzpatrick, W. Chen, G. S. Berenson, M. Barbieri, G. Paolisso, S. M. Gadalla, S. A. Savage, K. Christensen, A. I. Yashin, K. G. Arbeev, A. Aviv, Telomeres and the natural lifespan limit in humans. *Aging* **9**, 1130–1142 (2017).
34. Y. H. Choi, J.-K. Lim, M.-W. Jeong, K.-T. Kim, HnRNP A1 phosphorylated by VRK1 stimulates telomerase and its binding to telomeric DNA sequence. *Nucleic Acids Res.* **40**, 8499–8518 (2012).
35. F. M. Vega, A. Sevilla, P. A. Lazo, p53 Stabilization and accumulation induced by human vaccinia-related kinase 1. *Mol. Cell. Biol.* **24**, 10366–10380 (2004).
36. T. P. Molitor, P. Traktman, Depletion of the protein kinase VRK1 disrupts nuclear envelope morphology and leads to BAF retention on mitotic chromosomes. *Mol. Biol. Cell* **25**, 891–903 (2014).
37. A. Jamin, M. S. Wiebe, Barrier to autointegration factor (BANF1): Interwoven roles in nuclear structure, genome integrity, innate immunity, stress responses and progeria. *Curr. Opin. Cell Biol.* **34**, 61–68 (2015).
38. Y. S. Kim, S.-H. Kim, J. Shin, A. Harikishore, J.-K. Lim, Y. Jung, H.-N. Lyu, N.-I. Baek, K. Y. Choi, H. S. Yoon, K.-T. Kim, Luteolin suppresses cancer cell proliferation by targeting vaccinia-related kinase 1. *PLOS ONE* **9**, e109655 (2014).
39. A. Dillin, A.-L. Hsu, N. Arantes-Oliveira, J. Lehrer-Graiwer, H. Hsin, A. G. Fraser, R. S. Kamath, J. Ahringer, C. Kenyon, Rates of behavior and aging specified by mitochondrial function during development. *Science* **288**, 2398–2401 (2002).
40. S. S. Lee, R. Y. N. Lee, A. G. Fraser, R. S. Kamath, J. Ahringer, G. Ruvkun, A systematic RNAi screen identifies a critical role for mitochondria in *C. elegans* longevity. *Nat. Genet.* **33**, 40–48 (2003).

**Acknowledgments:** We thank I. Mattaj, V. Reinke, W. B. Mair, and A. Dillin for providing *C. elegans* strains and constructs. We thank D. Lee for helping generate *aak-2(T181A)::GFP* transgenic strain. We also thank Lee laboratory members and K. Kim for helpful discussions and valuable comments on the manuscript. We apologize to the authors whose papers were not cited in this manuscript because of the number limit. **Funding:** This research was supported by grants NRF-2019R1A3B2067745 and NRF-2017R1A5A1015366 funded by the Korean Government (MSIT) through the National Research Foundation (NRF) of Korea to S.-J.V.L. and by grant Basic Science Research Program (No. 2019R1A2C2009440) funded by the Korean Government (MSIT) through the NRF of Korea to K.-T.K. **Author contributions:** Conceptualization: M.A., S.P., S.H.H., K.-T.K., and S.-J.V.L. Investigation: M.A., S.P., S.H.H., H.-E.H.P., Y.J., A.B.H., W.S.S., and S.-J.V.L. Writing: M.A., S.P., and S.-J.V.L. Funding acquisition: S.-J.V.L. Supervision: K.-T.K. and S.-J.V.L. **Competing interests:** The authors declare that they have no competing interests. **Data and materials availability:** RNA-seq data have been deposited in Gene Expression Omnibus under accession code GSE138129. All data needed to evaluate the conclusions in the paper are present in the paper and/or the Supplementary Materials. Additional data related to this paper may be requested from the authors.

Submitted 30 January 2019
Accepted 18 May 2020
Published 1 July 2020
10.1126/sciadv.aaw7824

**Citation:** S. Park, M. Artan, S. H. Han, H.-E. H. Park, Y. Jung, A. B. Hwang, W. S. Shin, K.-T. Kim, S.-J. V. Lee, VRK-1 extends life span by activation of AMPK via phosphorylation. *Sci. Adv.* **6**, eaaw7824 (2020).